Ultrafast Electronic Phase Transition in $La_{1/2}Sr_{3/2}MnO_4$ by Coherent Vibrational Excitation: Evidence for Nonthermal Melting of Orbital Order

R. I. Tobey,[1] D. Prabhakaran,[1] A. T. Boothroyd,[1] and A. Cavalleri[1,2]
[1]*Department of Physics, University of Oxford, Oxford, United Kingdom*
[2]*Max Planck Group for Structural Dynamics–University of Hamburg–CFEL, Hamburg, Germany*
(Received 29 April 2008; published 6 November 2008)

An ultrafast electronic phase transition, associated with melting of orbital order, is driven in $La_{1/2}Sr_{3/2}MnO_4$ by selectively exciting the Mn-O stretching mode with femtosecond pulses at 16 μm wavelength. The energy coupled into this vibration is less than 1% of that necessary to induce the transition thermally. Nonthermal melting of this electronic phase originates from coherent lattice displacements comparable to the static Jahn-Teller distortion.

DOI: 10.1103/PhysRevLett.101.197404 PACS numbers: 78.47.−p, 71.30.+h

Manganites exhibit extreme sensitivity to external perturbations, such as magnetic [1] and electric fields [2], pressure [3], photoexcitation with x rays [4], or visible radiation [5–7]. Recently, we have shown that an insulator-metal transition can also be driven in $Pr_{0.7}Ca_{0.3}MnO_3$ when a Mn-O stretching vibration is selectively excited with midinfrared radiation [8]. A direct connection could then be drawn between this lattice distortion and the electronic phase of the solid. We posited that large-amplitude lattice distortions modulated the tolerance factor and crystal field splitting of the perovskite lattice structure, increasing the electron hopping probability and inducing the metallic phase. However, the underlying dynamics of charge, spin, and orbital degrees of freedom, which are innately connected to the conductivity changes, could not be probed directly in the optical properties.

In this Letter we report on a study of $La_{1/2}Sr_{3/2}MnO_4$, a half-doped, single-layer system in which long-range homogeneous electronic and orbital structure can be directly connected to the macroscopic optical properties. We measure ultrafast reflectivity over a broad spectral range, and we detect the formation of a long-lived electronic phase with transient optical properties similar to those observed in the high-temperature, orbitally melted insulator. The occurrence of ultrafast melting of orbital order is further substantiated by the prompt loss of birefringence, which we measure with femtosecond pulses at 650 nm. Importantly, the energy deposited into the solid accounts for only minimal heating. We thus conclude that selective vibrational excitation drives the transition nonthermally.

Figure 1(a) shows the three dimensional lattice structure of single-layer $La_{1/2}Sr_{3/2}MnO_4$. The manganese cations occupy the center of oxygen octahedra forming planes separated by lanthanum and strontium dopants. Within the planes, ordering of the Mn $3d$ e_g-like orbitals develops below $T_{00} = 220$ K, yielding a long-range pattern as shown in Fig. 1(b). This low-temperature orbital configuration breaks the tetragonal lattice symmetry and results in optical birefringence—a rotation of the polarization of an optical probe when this is not aligned to either principle axis. The electronic properties are dominated by the crystal-field-split Mn $3d$ orbitals, which are strongly hybridized with $2p$ orbitals from neighboring oxygen atoms, and are thus very sensitive to distortions in the Mn-O bond.

In our experiments, large-amplitude, coherent distortions of the Mn-O bonds were driven with femtosecond pulses at 16 μm (625 cm^{-1}, 77 meV) wavelength, resonant with the IR-active, 625 cm^{-1} stretching vibration. High-intensity pulses at this wavelength were generated with an optical parametric amplifier, which was pumped by a Ti:sapphire laser generating 2.5 mJ pulses at 1 kHz repetition rate. The maximum fluence in the mid-IR was 2 mJ/cm^2. A second optical parametric amplifier, pumped by the same laser, was used to generate broadband probe pulses, which in our experiments were tuned between 10 μm (0. 12 eV photon energy) and 600 nm (2.2 eV). The single crystal samples were grown by the floating zone technique, cleaved and polished along [001], and mounted in a closed loop cryostat.

The top panel of Fig. 2 shows the IR driven time-dependent reflectivity of $La_{1/2}Sr_{3/2}MnO_4$ at 650 nm, measured at a temperature of 90 K, below the orbital ordering temperature. We find a prompt transition to a long-lived phase that survives for hundreds of picoseconds after excitation. The same process probed at other wavelengths in the infrared yielded qualitatively similar temporal profiles. The transient changes in reflectivity, measured at 100-ps time delay, are shown in the middle panel of Fig. 2 for photon energies between 120 meV and 2.2 eV. We observe an increase in reflectivity at all measured photon energies below 1 eV.

The bottom panel of Fig. 2 shows the static reflectivity of $La_{1/2}Sr_{3/2}MnO_4$, measured at 90 K, 110 K, and at room temperature. Below $T_{00} = 220$ K, the static reflectivity exhibits a resonance near 1.3 eV, corresponding to intersite excitations between adjacent manganese atoms, reflecting the cooperative, long-range Jahn-Teller distortion. Above T_{00}, this feature is lost and spectral weight shifts to lower

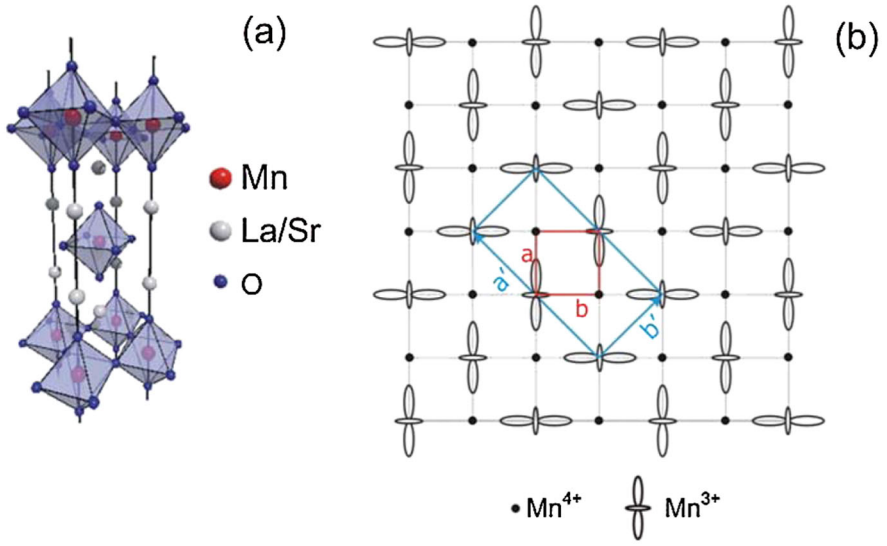

FIG. 1 (color online). Structure of $La_{1/2}Sr_{3/2}MnO_4$. (a) Three dimensional structure of single-layer $La_{1/2}Sr_{3/2}MnO_4$ consists of planes of oxygen octahedra separated by lanthanum and strontium dopants. A manganese atom occupies the center of the oxygen octahedra. (b) Below $T_{00} = 220$ K, lattice-commensurate orbital ordering of Mn $3d$ e_g-like breaks the symmetry of the tetragonal lattice and results in optical birefringence. Near-edge optical properties derived from electronic hopping between adjacent Mn $3d$ atomic orbitals via hybridization with intermediate oxygen atoms.

energies. A comparison between reflectivity changes obtained by vibrational excitation and by static temperature tuning is also shown in the middle panel of Fig. 2. We note that the spectral response of the transient phase is the same as the change in static reflectivity when $La_{1/2}Sr_{3/2}MnO_4$ is heated between 90 K and room temperature, suggesting a similarity between the two phases.

Despite good qualitative matching, the absolute size of the transient reflectivity change is nearly 2 orders of magnitude smaller than that induced thermally. However, it is also important that the spectral response cannot be reconciled with changes observed for smaller temperature increases. This is shown by the 110–90 K differential reflectivity (dashed line in Fig. 2), where the sample remains in the orbitally ordered phase. We conclude that vibrational excitation only converts a fraction of the volume, creating domains of vibrationally induced product within the parent phase. By scaling this value by the mismatch in pump and probe depths, we estimate that the filling factor is approximately 5%. We expect complete transformation for higher excitation energies, not possible with the laser power used here.

The spectral response (Fig. 2, middle) suggests that vibrational excitation relaxes the Jahn-Teller-distorted low-temperature state [9] and leads to a metastable phase where orbital order is melted. Ultrafast loss of orbital ordering can be directly confirmed by measuring time-dependent birefringence [10], which at 650 nm is proportional to the orbital-order parameter, as measured with resonant x-ray diffraction [11]. For the sake of consistency, we measure this quantity in the same way as defined in Refs. [10,11], i.e., as the normalized differential reflectiv-

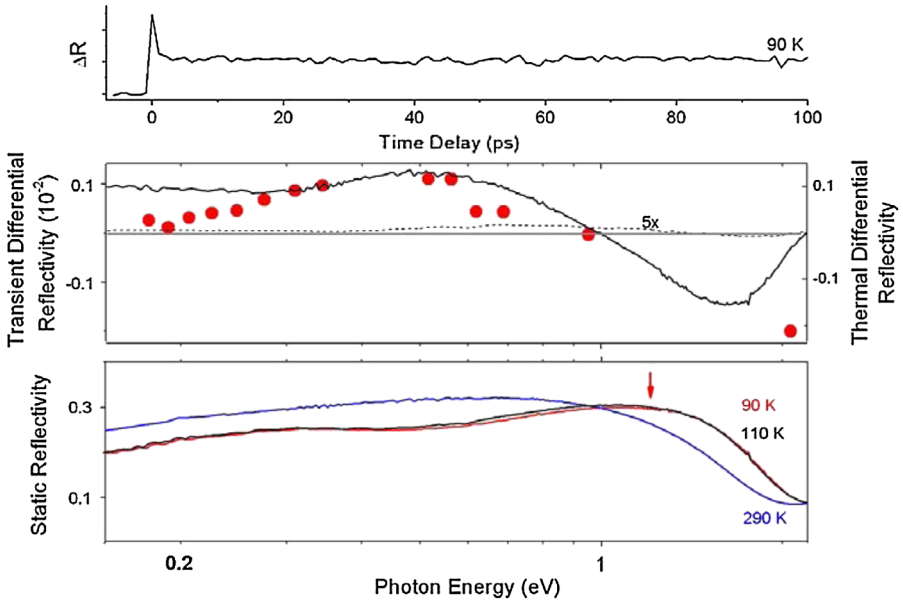

FIG. 2 (color online). Static and transient reflectivity spectra. Top: The vibrationally induced changes in reflectivity at 90 K, probed at 650 nm, reveal a prompt and long-lived product phase. Middle: The spectral response at 100 ps time delay (data points) closely corresponds to the observed changes in reflectivity when the sample is heated above T_{00} (solid line), but not when the sample temperature is increased by 20 K (dashed line). Bottom: The spectral feature at 1.3 eV (arrow) is associated with orbital ordering. Above T_{00} (290 K), spectral weight shifts to lower energies.

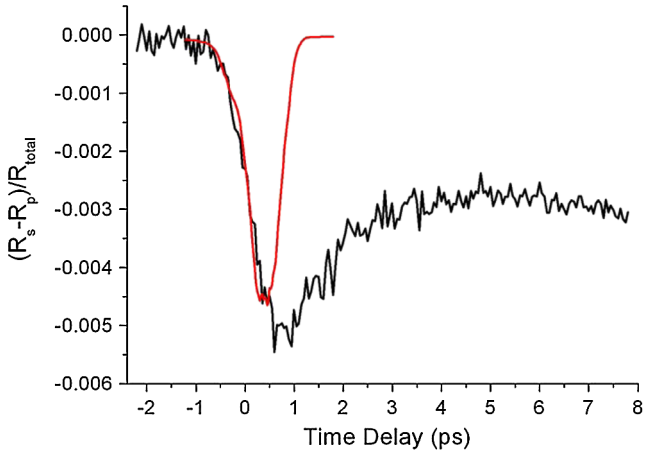

FIG. 3 (color online). Ultrafast loss of birefringence. Selective excitation of the vibrational resonance at 80 meV results in the prompt destruction of orbital ordering and a loss of birefringence at 650 nm (black line). A cross correlation [gray (red) line] of the mid-IR pump and 650 nm indicates that melting occurs within the pulse width of the pump.

ity between s and p polarizations when the incident electric field is aligned at 45° from the two principal axes of the orbital crystal (see Fig. 1). Figure 3 shows time-dependent birefringence, as measured at 650 nm after the same vibrational excitation. A prompt drop in birefringence is observed, directly indicating melting of orbital order. This state persists for hundreds of picoseconds. In Fig. 3, we also include a cross correlation of mid-IR pump and 650-nm probe pulses, as measured with the Kerr effect in ZnTe. The data show that birefringence is lost on a time scale identical to the rise time of the excitation pulse, indicative of the ultrafast nature of this process. This is the first indication that the electronic phase transition is nonthermal, in that it occurs on a time scale that is significantly shorter than the known thermalization time for hot optical phonons in solids [12]. Yet, important details of the excitation mechanism are lost in our experiments. The lack of carrier-envelope phase stability results in excitation of lattice vibrations with different absolute phases for subsequent pump pulses, and the signature of the electric field is lost by averaging over many pump-probe cycles.

In Fig. 4 we plot the inverse of the threshold fluence [13] against photon energy, exhibiting a sharp increase in efficiency below 100 meV, i.e., where absorption by optical phonon excitation sets in. For comparison, we also show the linear infrared absorption profile over the same range of pump energies. We find that the inverse threshold peaks at the position of the Mn-O stretching mode, but we cannot assess in any more detail the specific role of individual normal modes of the lattice. This is due to a combination of the broad spectrum of our ultrashort midinfrared pulses and strongly decreasing generation efficiencies for wavelengths longer than 18 μm. Excitation at photon energies above the vibrational resonances still results in reflectivity changes, although the threshold increases by nearly 2 orders of magnitude already at 110 meV. Excitation of the electronic phase transition away from the absorption peak is likely the result of nonresonant coupling to the same 80-meV vibration, and possibly of the excitation of a coherent phonon-polariton mode, a mixture of lattice vibrations and propagating electromagnetic radiation. The threshold increases because the mechanical energy coupled into the mode decreases as the frequency is tuned away from the resonance [14–16].

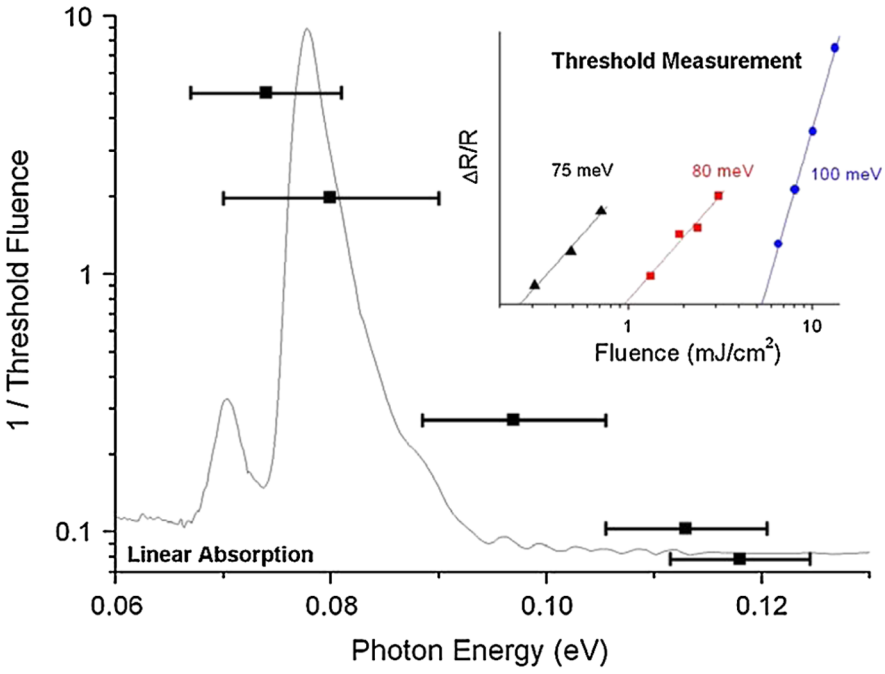

FIG. 4 (color online). Threshold behavior. As the pump wavelength is tuned to resonance the threshold fluence drops dramatically. The central photon energy is shown and the horizontal bars represent the full width at half maximum of the pump bandwidth measured using linear interferometric autocorrelation. The complex part of the index of refraction is shown as a guide for the eye (solid line). Inset shows threshold behavior for three pump photon energies.

Importantly, the observed effects cannot be explained by heating of $La_{1/2}Sr_{3/2}MnO_4$ above $T_{00} \sim 220$ K. At 16 μm, we use fluences between the 0.2-mJ/cm^2 threshold and 2 mJ/cm^2, corresponding to energy densities below 6 kJ/cm^3 over the 300 nm absorption depth. At equilibrium, this corresponds to heating of less than 2 K. However, Fig. 3 shows that orbital order is lost at the earliest times, when the energy is deposited into only one, or at most, a few strongly coupled modes of the lattice. These have a high temperature and large-amplitude oscillations, while the lattice has not reached thermal equilibrium.

Taking a complementary view of the excitation process, we note that the peak electric-field amplitude during the pulse is nearly 10 MV/cm. Assuming ionic bonding between $Mn^{3.5+}$ and O^{2-} ions, and deriving a value for the polarizability ($P = \varepsilon_0 \chi E$) from the dielectric constant at this frequency [$\chi(\omega_0) = \varepsilon(\omega_0) - 1$], we estimate a coherently driven lattice displacement between 2 and 10 pm ($d = P/nQ$, where n is the density of Mn-O dipoles and $Q \sim 5.5e^-$). This quantity is about 1%–5% of the equilibrium Mn-O distance. This uncertainty derives from various unknown quantities, such as an amplitude-dependent polarizability of the lattice, fluctuations in the valency of the individual ions, and possibly a time-dependent, nonlinear reflection and absorption of the pump. The estimated field-induced displacement is comparable to the static Jahn-Teller distortion, which for manganites is about 10 pm [9]. We conclude that selective vibrational excitation destabilizes the charge and orbitally ordered state of low-temperature $La_{1/2}Sr_{3/2}MnO_4$ by electric-field induced coherent displacements rather then by heating of the solid.

It is interesting to note that the dynamics of the optical properties of the vibrationally driven transition reported here closely resemble what is also observed in photodoping experiments [10]. This observation is very revealing. Photodoping experiments trigger large-amplitude coherent lattice distortions as well as changes in electronic occupancy [7], and thus both the bandwidth of the system (or the hopping amplitude, t) and the filling (number of electrons per site) are perturbed simultaneously. It is then difficult to identify which of the two perturbations triggers the macroscopic switching of the electronic properties.

In the present case, the filling is left unperturbed, while only the bandwidth is modulated, allowing for a direct assignment of the microscopic cause of the orbital melting. One is then tempted to conclude that lattice distortions are the true underlying cause of ultrafast orbital melting and that photodoping in manganites only couples to the electronic structure indirectly through the excitation of lattice distortions.

In summary, we have shown mode selective excitation of an orbital melting transition in single-layer $La_{1/2}Sr_{3/2}MnO_4$. The electronic phase transition is detected by measuring a prompt change in the mid-IR optical properties and in the ultrafast loss of birefringence. The transition is spectrally selective and efficiently driven when the pump frequency matches that of the 625 cm^{-1} stretching vibration. The transition is nonthermally driven by coherent atomic displacements comparable to the Jahn-Teller distortion. In the future, excitation by carrier-envelope phase stable pulses will allow for direct measurements of the coherent lattice displacements at the earliest time delays. Additionally, these techniques show promise in coherently driving transitions in copper oxide superconductors which share many structural elements with manganites.

The authors would like to thank T. Ishikawa for static reflectivity measurements.

[1] M. B. Salamon and M. Jaime, Rev. Mod. Phys. **73**, 583 (2001).
[2] A. Asamitsu, Y. Tomioka, H. Kuwahara, and Y. Tokura, Nature (London) **388**, 50 (1997).
[3] H. Y. Hwang, T. T. M. Palstra, S. W. Cheong, and B. Batlogg, Phys. Rev. B **52**, 15 046 (1995).
[4] V. Kiriukhin *et al.*, Nature (London) **386**, 813 (1997).
[5] K. Miyano, T. Tanaka, Y. Tomioka, and Y. Tokura, Phys. Rev. Lett. **78**, 4257 (1997).
[6] M. Fiebig, K. Miyano, Y. Tomioka, and Y. Tokura, Appl. Phys. B **71**, 211 (2000).
[7] D. Polli *et al.*, Nature Mater. **6**, 643 (2007).
[8] M. Rini *et al.*, Nature (London) **449**, 72 (2007).
[9] S. Satpathy, Z. Popovic, and F. Vukajlovic, Phys. Rev. Lett. **76**, 960 (1996).
[10] T. Ogasawara *et al.*, Phys. Rev. B **63**, 113105 (2001).
[11] T. Ishikawa, K. Ookura, and Y. Tokura, Phys. Rev. B **59**, 8367 (1999).
[12] D. von der Linde, J. Kuhl, and H. Klingenberg, Phys. Rev. Lett. **44**, 1505 (1980).
[13] J. M. Liu, Opt. Lett. **7**, 196 (1982).
[14] T. P. Dougherty, G. P. Wiederrecht, K. A. Nelson, M. Garret, H. P. Jannsen, and C. Warde, Phys. Rev. B **50**, 8996 (1994).
[15] J. K. Wahlstrand and R. Merlin Phys. Rev. B **68**, 054301 (2003).
[16] A. Cavalleri *et al.*, Nature (London) **442**, 664 (2006).